

NACA TN 4258 66501

0066797



TECH LIBRARY KAFB, NM

NATIONAL ADVISORY COMMITTEE FOR AERONAUTICS

TECHNICAL NOTE 4258

A NUMERICAL METHOD FOR EVALUATING WAVE DRAG

By Maurice S. Cahn and Walter B. Olstad

Langley Aeronautical Laboratory
Langley Field, Va.



Washington

June 1958

AFM2C
TECHNICAL LIBRARY
AFL 2811



0066797

NATIONAL ADVISORY COMMITTEE FOR AERONAUTICS

TECHNICAL NOTE 4258

A NUMERICAL METHOD FOR EVALUATING WAVE DRAG

By Maurice S. Cahn and Walter B. Olstad

SUMMARY

A numerical method for evaluating the Von Kármán wave-drag equation has been developed and applied to the calculation of wave drag for several bodies of revolution. Results indicated good agreement with the exact solution. Sufficient accuracy of wave drag was obtained by using a simple numerical method to determine the second derivatives of the area distributions.

It is concluded that the numerical method will yield results well within the accuracy of linearized theory. The method may be set up easily for a desk calculator or an electronic computer.

INTRODUCTION

Area-rule concepts (ref. 1) have shown that the wave drag of a configuration is related to the wave drag of an equivalent body of revolution. As a result, much interest has been directed toward the evaluation of the wave drag of bodies of revolution. The most common method of approach has been to evaluate the Von Kármán wave-drag formula with a Fourier series analysis. This method is outlined in reference 2. It would seem that a method of numerically evaluating the double integral in the Von Kármán equation might, in some cases, be more useful to the engineer. Such a method is devised and presented in this report.

SYMBOLS

C_D	wave-drag coefficient, $\frac{\text{Wave drag}}{qS_F}$
D	wave drag
i	index of summation in x

j	index of summation in $x - \xi$
L_j	defined by equation (4)
l	body length
M	free-stream Mach number
n	number of terms of summation
q	dynamic pressure
r	body radius
R	body maximum radius of configuration 1
S	body cross-sectional area
S_f	body frontal area of configuration 1
x	coordinate of longitudinal axis of body

$$\beta = \sqrt{M^2 - 1}$$

ξ auxiliary coordinate of longitudinal axis of body

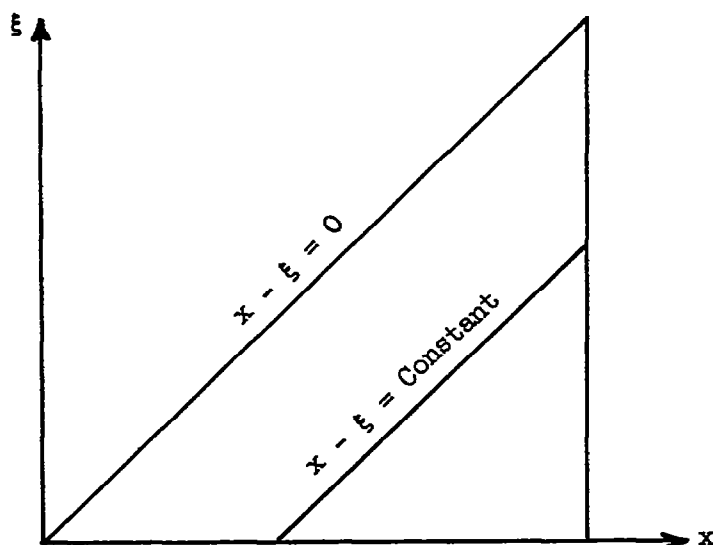
Primes indicate derivatives with respect to the argument.

ANALYSIS

The Von Kármán wave-drag equation for a body of revolution as given in reference 3 can be presented in the form

$$\frac{D}{q} = -\frac{1}{\pi} \int_0^l \int_0^x S''(x) S''(\xi) \log(x - \xi) d\xi dx \quad (1)$$

The integral in equation (1) may be considered as the volume between a surface determined by the function $S''(x) S''(\xi) \log(x - \xi)$ and the x, ξ plane. The volume is bounded laterally by the planes $\xi = 0$, $x = l$, and $x = \xi$, as shown in the following sketch:



Along any line $x - \xi = \text{Constant}$, the term $\log(x - \xi)$ is a constant. Thus, if the integration proceeds first along this line, the term $\log(x - \xi)$ may be taken outside of the integral sign. The second integration is then performed with respect to $(x - \xi)$ from 0 to l .

From these considerations, a numerical solution to equation (1) can be somewhat simplified. The x, ξ plane can be divided into a number of finite diagonal strips of equal width, and values of $S''(x)S''(\xi)$ along the center of each strip can be computed. These values then are summed along the strips for which $x - \xi = \text{Constant}$ and multiplied by the value of $\log(x - \xi)$ integrated across the strip. Using the integrated value of $\log(x - \xi)$ over the strip rather than the value of the logarithm itself avoids the problem of the singularity on the line $x = \xi$. It should be noted here that the summation for the line $x = \xi$ is divided by 2 so that no areas outside of the limits of the integration are included. Finally, the products of the summation along each line for which $x - \xi = \text{Constant}$ and the integrated value of $\log(x - \xi)$ are summed to obtain the solution. This integration is thus described by the following expression:

$$\frac{D}{q} = -\frac{l^2}{\pi n^2} \sum_{j=0}^{n-1} L_j \sum_{i=j}^{n-1} S''_i S''_{i-j} \quad (2)$$

where $S_1'' = S'' \left[\frac{l}{n} \left(1 + \frac{1}{2} \right) \right]$ for the examples herein, and

$$\left. \begin{aligned} L_j &= \frac{n}{l} \int_{\left(j - \frac{1}{2}\right) \frac{l}{n}}^{\left(j + \frac{1}{2}\right) \frac{l}{n}} \log(x - \xi) d(x - \xi) \\ L_j &= \left[\left(j + \frac{1}{2}\right) \log \left(j + \frac{1}{2}\right) - \left(j - \frac{1}{2}\right) \log \left(j - \frac{1}{2}\right) \right] + \left(\log \frac{l}{n} - 1 \right) \end{aligned} \right\} \quad (3)$$

Since $S'(0) = S'(l) = 0$,

$$\int_0^l \int_0^x S''(x) S''(\xi) d\xi dx = \frac{1}{2} [S'(l) - S'(0)]^2 = 0$$

Therefore the constant term $\left(\log \frac{l}{n} - 1 \right)$ in L_j can be eliminated, with the result that

$$L_j = \left(j + \frac{1}{2}\right) \log \left(j + \frac{1}{2}\right) - \left(j - \frac{1}{2}\right) \log \left(j - \frac{1}{2}\right) \quad (4)$$

When $j = 0$, $L_0 = \frac{1}{2} \log \frac{1}{2}$.

Equation (4) is independent of both the number and the size of increments and can be used whenever $S'(0) = S'(l) = 0$. Values of the function L_j for j from 0 to 99 are presented in table I.

When $S'(l)$ is not equal to zero, the term $\left(\log \frac{l}{n} - 1 \right)$ must be retained in L_j , and additional terms must be used with Von Kármán's equation (see ref. 4). These terms are

$$\frac{[S'(l)]^2}{2\pi} \log \frac{2}{\pi r(l)} + \frac{S'(l)}{\pi} \int_0^l S''(x) \log(l - x) dx \quad (5)$$

The integral in equation (5) can be evaluated with a single numerical summation by utilizing the information already obtained in the evaluation of equation (1).

DISCUSSION

In order to determine the accuracy of this numerical method, the wave drag of an analytical body of revolution was computed by this method, with the $\frac{x}{l}$ - and $\frac{z}{l}$ -axes each divided into 40 equal increments, and by analytic integration of Von Kármán's equation. The shape of the analytical body (configuration 1) was given by the following expression:

$$\frac{r}{R} = 4 \left[\left(\frac{x}{l} \right) - \left(\frac{x}{l} \right)^2 \right]$$

In order to test the accuracy of the numerical procedure, exact values of the second derivative of the area distribution S'' were used. The value of the wave-drag coefficient obtained by the numerical method was $42.648 \left(\frac{R}{l} \right)^2$ as compared with the exact value of $42.667 \left(\frac{R}{l} \right)^2$, a difference of 0.045 percent. A layout of the calculations involved in the numerical method is presented in table II.

The wave drag for configuration 1 was also determined numerically by using 100 increments. Again, exact values of S'' were used. The value of the wave-drag coefficient obtained from these calculations was $42.523 \left(\frac{R}{l} \right)^2$, a difference of 0.337 percent from the exact value.

In practical applications of the numerical method, the exact values of the second derivative of the area distributions would not be available. In fact, the exact area distribution is not generally known. Thus, evaluation of the second derivative by various numerical procedures may lead to considerable error. These errors, in turn, may have a large effect on the accuracy of the numerical method for evaluating wave drag. In order to determine this effect, three additional bodies of revolution were developed for which the exact values of S'' were known. These bodies have large variations of curvature of their area distributions in order to provide a severe test. Configuration 2 was obtained by adding $0.25 \left[1 + \cos 10\pi \left(\frac{x}{l} - 0.5 \right) \right]$ for $0.4 \leq \frac{x}{l} \leq 0.6$ to the nondimensional area distribution of configuration 1 (the parabolic body of revolution described previously). Configuration 3 was obtained by subtracting this term from the nondimensional area distribution of configuration 1. Configuration 4 was obtained by adding $0.25 \left[1 + \cos 10\pi \left(\frac{x}{l} - 0.4 \right) \right]$ for $0.3 \leq \frac{x}{l} \leq 0.7$ to the nondimensional

area distribution of configuration 1. These area distributions (see fig. 1) were plotted to a scale commensurate with the accuracy of the area distribution of a typical wind-tunnel model. Values of the second derivatives were then obtained by picking values of area from the curves and substituting them into the formula

$$S_1'' = \frac{S_{i-1} - 2S_i + S_{i+1}}{(l/n)^2}$$

where $n = 100$. A comparison of these approximate values of S'' with exact values is presented in figure 2 for configuration 3. Values of wave-drag coefficient were computed for the four bodies by the numerical method (for 100 increments) by using first, the exact values of S'' , and second, the approximate values. A comparison of the results is shown in the following table:

Configuration	C_D for -		Percent difference
	Exact S''	Approximate S''	
1	$42.523\left(\frac{R}{l}\right)^2$	$42.655\left(\frac{R}{l}\right)^2$	0.31
2	$329.234\left(\frac{R}{l}\right)^2$	$325.815\left(\frac{R}{l}\right)^2$	1.04
3	$303.255\left(\frac{R}{l}\right)^2$	$296.848\left(\frac{R}{l}\right)^2$	2.12
4	$642.438\left(\frac{R}{l}\right)^2$	$645.949\left(\frac{R}{l}\right)^2$.55

Despite the relatively large errors in some of the individual approximate values of S'' (see fig. 2), the values of wave-drag coefficient computed from these values were in close agreement with those computed from the exact values of S'' . These results are not surprising when it is considered that the approximate values of S'' form a set of exact values of the second derivative of an area distribution which differs little from the original area distribution. The differences between the two area distributions will be of the same order of magnitude as the accuracy to which the original area distribution is known. Obviously the wave drag determined by these two area distributions will be approximately the same. Any differences will be well within the accuracy by which the theory can be expected to apply to a practical example.

The examples cited in the previous paragraphs indicate that 100 increments are sufficient to yield good accuracy in the evaluation of wave drag. A larger number of increments might be used for an area distribution which has even more rapid changes in shape than those studied herein. However, it should be kept in mind that a body with such an area distribution will not permit linearized flow approximation, and equation (1) should not be expected to yield good agreement with experiment. In fact, if the slope of the area distribution is discontinuous, Von Kármán's equation indicates an infinite value for the wave drag, which obviously disagrees with experimental evidence.

It should be noted that the technique developed herein can be readily adapted to the evaluation of the wave drag of lifting configurations (see ref. 5) and to vortex drag of a lifting surface in subsonic or supersonic flow (see ref. 4).

CONCLUDING REMARKS

A numerical method has been developed for evaluating Von Kármán's wave-drag equation. The method may be set up easily for a desk calculator or an electronic computer and will yield results well within the accuracy of linearized theory. A simple numerical method was used for determining the second derivatives of nonanalytic area distributions for four bodies of revolution. Results of calculations made by using these approximate derivatives and by using exact derivatives yielded differences in wave drag on the order of 2 percent for a practical case.

The numerical method developed herein can be adapted to the evaluation of the wave drag of lifting configurations and to the vortex drag of a lifting surface in subsonic or supersonic flow.

Langley Aeronautical Laboratory,
National Advisory Committee for Aeronautics,
Langley Field, Va., February 28, 1958.

REFERENCES

1. Whitcomb, Richard T.: A Study of the Zero-Lift Drag-Rise Characteristics of Wing-Body Combinations Near the Speed of Sound. NACA Rep. 1273, 1956. (Supersedes NACA RM L52H08.)
2. Holdaway, George H.: Comparison of Theoretical and Experimental Zero-Lift Drag-Rise Characteristics of Wing-Body-Tail Combinations Near the Speed of Sound. NACA RM A53H17, 1953.
3. Hayes, Wallace D.: Linearized Supersonic Flow. Rep. No. AL-222, North American Aviation, Inc., June 18, 1947.
4. Heaslet, Max. A., and Lomax, Harvard: Supersonic and Transonic Small Perturbation Theory. General Theory of High-Speed Aerodynamics. Vol. VI of High Speed Aerodynamics and Jet Propulsion, sec. D., W. R. Sears, ed., Princeton Univ. Press, 1954, pp. 122-344.
5. Lomax, Harvard: The Wave Drag of Arbitrary Configurations in Linearized Flow As Determined by Areas and Forces in Oblique Planes. NACA RM A55A18, 1956.

TABLE I.- VALUES OF THE FUNCTION L_j FOR j FROM 0 TO 99

j	L_j	j	L_j	j	L_j
0	-0.3470	34	4.5265	68	5.2191
1	.9547	35	4.5552	69	5.2346
2	1.6825	36	4.5835	70	5.2481
3	2.0939	37	4.6109	71	5.2631
4	2.3837	38	4.6377	72	5.2767
5	2.6078	39	4.6635	73	5.2898
6	2.7906	40	4.6888	74	5.3045
7	2.9451	41	4.7135	75	5.3172
8	3.0788	42	4.7376	76	5.3309
9	3.1967	43	4.7613	77	5.3440
10	3.3022	44	4.7843	78	5.3567
11	3.3975	45	4.8065	79	5.3696
12	3.4846	46	4.8286	80	5.3820
13	3.5648	47	4.8503	81	5.3940
14	3.6387	48	4.8710	82	5.4071
15	3.7080	49	4.8919	83	5.4190
16	3.7724	50	4.9120	84	5.4304
17	3.8331	51	4.9319	85	5.4431
18	3.8903	52	4.9512	86	5.4537
19	3.9443	53	4.9704	87	5.4664
20	3.9956	54	4.9890	88	5.4770
21	4.0445	55	5.0072	89	5.4890
22	4.0909	56	5.0255	90	5.4997
23	4.1355	57	5.0428	91	5.5109
24	4.1779	58	5.0609	92	5.5218
25	4.2189	59	5.0776	93	5.5323
26	4.2579	60	5.0939	94	5.5435
27	4.2958	61	5.1113	95	5.5542
28	4.3322	62	5.1272	96	5.5637
29	4.3674	63	5.1429	97	5.5748
30	4.4010	64	5.1585	98	5.5855
31	4.4342	65	5.1747	99	5.5950
32	4.4656	66	5.1895		
33	4.4963	67	5.2050		

TABLE II. - SAMPLE CALCULATIONS FOR PARABOLIC BODY OF REVOLUTION

[In making the calculations values of S'' with seven decimal places were used, but for convenience of tabulation they have been rounded to four places.]

j	S''(x)	S''(t)S''(x)																						
		1=0	1=1	1=2	1=3	1=4	1=5	1=6	1=7	1=8	1=9	1=10	1=11	1=12	1=13	1=14	1=15	1=16	1=17	1=18	1=19	1=20	1=21	1=22
29	.9259	.8974	.7834	.6484	.5209	.4009	.2884	.1834	.0859	-.0041	-.0866	-.1616	-.2291	-.2891	-.3416	-.3866	-.4241	-.4541	-.4766	-.4916	-.4991	-.4991	-.4916	-.4766
28	.7834		.7254	.5004	.4824	.3712	.2671	.1699	.0796	-.0038	-.0802	-.1496	-.2122	-.2677	-.3163	-.3579	-.3927	-.4204	-.4413	-.4552	-.4621	-.4621	-.4552	-.4413
27	.6484		.6136	.4084	.3141	.2260	.1457	.0672	-.0032	-.0678	-.1266	-.1795	-.2269	-.2676	-.3068	-.3422	-.3727	-.3974	-.4161	-.4287	-.4340	-.4340	-.4287	-.4161
26	.5004			.4205	.2600	.1870	.1189	.0527	-.0026	-.0561	-.1048	-.1485	-.1874	-.2215	-.2507	-.2750	-.2944	-.3090	-.3187	-.3236	-.3236	-.3187	-.3090	-.2944
25	.4009				.2099	.1503	.0956	.0448	-.0021	-.0451	-.0842	-.1195	-.1506	-.1779	-.2014	-.2209	-.2365	-.2483	-.2561	-.2600	-.2600	-.2561	-.2483	-.2365
24	.3141					.1608	.1156	.0735	.0245	-.0016	-.0347	-.0648	-.0918	-.1159	-.1369	-.1550	-.1700	-.1821	-.1911	-.1971	-.2001	-.2001	-.1971	-.1911
23	.2260						.0832	.0529	.0248	-.0012	-.0250	-.0466	-.0661	-.0834	-.0985	-.1115	-.1225	-.1310	-.1375	-.1416	-.1439	-.1439	-.1416	-.1375
22	.1457							.0536	.0245	-.0007	-.0159	-.0296	-.0420	-.0530	-.0627	-.0709	-.0778	-.0833	-.0874	-.0902	-.0915	-.0915	-.0902	-.0874
21	.0672								.0074	-.0005	-.0074	-.0139	-.0197	-.0248	-.0294	-.0332	-.0364	-.0390	-.0410	-.0422	-.0429	-.0429	-.0422	-.0410
20	.0056									.0004	-.0007	-.0009	-.0012	-.0014	-.0016	-.0017	-.0018	-.0019	-.0019	-.0020	-.0020	-.0020	-.0020	-.0019
19	-.0802										.0004	.0140	.0196	.0250	.0296	.0332	.0364	.0390	.0410	.0422	.0429	.0429	.0422	.0410
18	-.1616											.0140	.0196	.0250	.0296	.0332	.0364	.0390	.0410	.0422	.0429	.0429	.0422	.0410
17	-.2291												.0140	.0196	.0250	.0296	.0332	.0364	.0390	.0410	.0422	.0429	.0429	.0422
16	-.2891													.0140	.0196	.0250	.0296	.0332	.0364	.0390	.0410	.0422	.0429	.0429
15	-.3416														.0140	.0196	.0250	.0296	.0332	.0364	.0390	.0410	.0422	.0429
14	-.3866															.0140	.0196	.0250	.0296	.0332	.0364	.0390	.0410	.0422
13	-.4241																.0140	.0196	.0250	.0296	.0332	.0364	.0390	.0410
12	-.4541																	.0140	.0196	.0250	.0296	.0332	.0364	.0390
11	-.4766																		.0140	.0196	.0250	.0296	.0332	.0364
10	-.4916																			.0140	.0196	.0250	.0296	.0332
9	-.4991																				.0140	.0196	.0250	.0296
8	-.4991																					.0140	.0196	.0250
7	-.4916																						.0140	.0196
6	-.4766																							.0140
5	-.4541																							.0140
4	-.4241																							.0140
3	-.3866																							.0140
2	-.3416																							.0140
1	-.2891																							.0140
0	-.2291																							.0140

$$C_D = -\left(\frac{2\pi}{\ln 1}\right)^2 \sum_{j=0}^{n-1} L_j \sum_{i=j}^{n-1} S_i'' S_{i-1}''$$

therefore

$$C_D = 42.649 \left(\frac{R}{l}\right)^2$$

$$C_D = -\frac{(2\pi R)}{n!} \sum_{j=0}^{n-1} I_j \sum_{i=j}^{n-1} S_i'' S_{i-1}''$$

therefore

$$C_D = 42.648 \left(\frac{R}{l}\right)^2$$

$$\sum_{j=0}^{N-1} L_j \sum_{i=j}^{N-1} s_i^* s_{i-j}^* = -66.6374$$

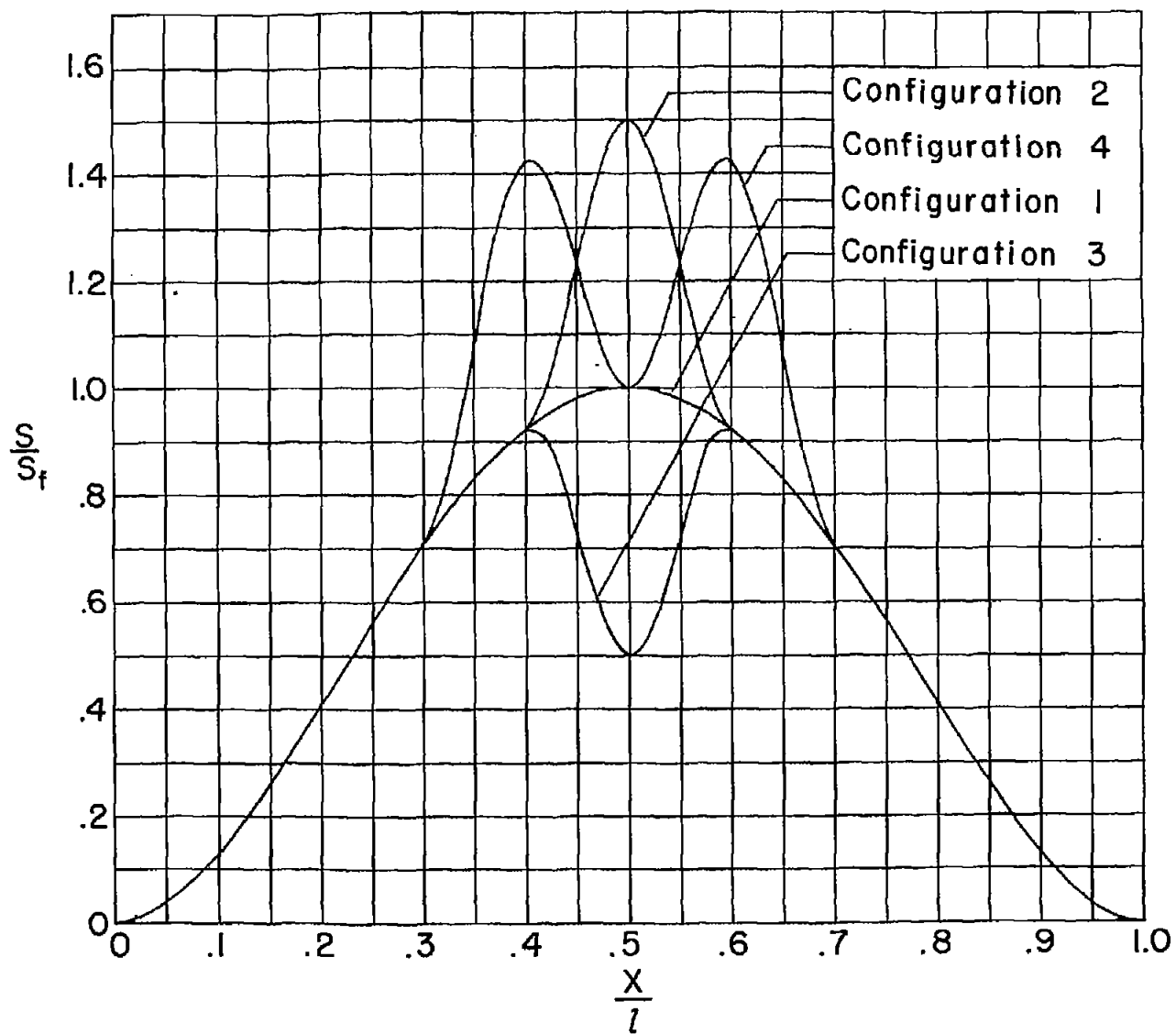


Figure 1.- Area distributions for four bodies of revolution.

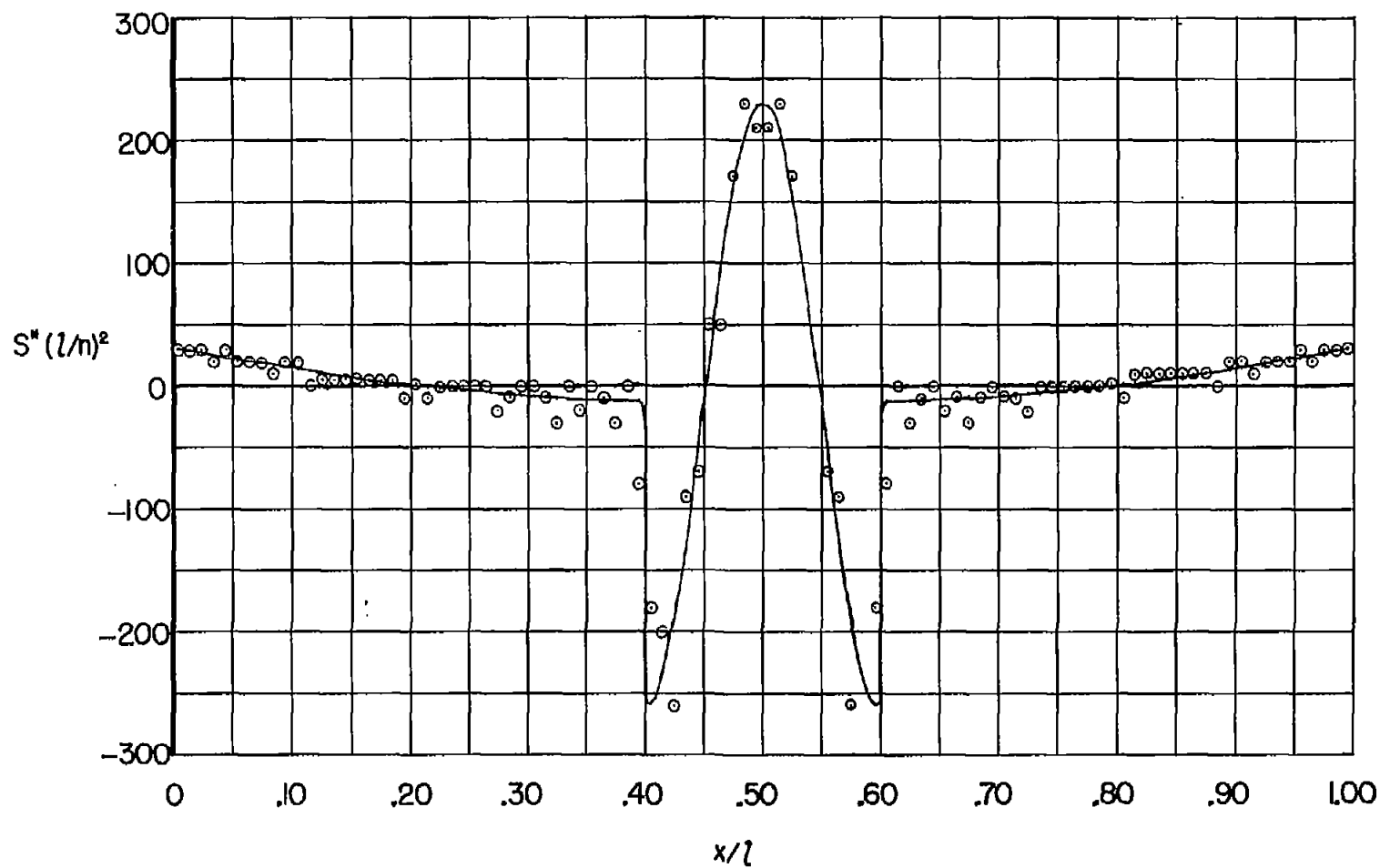


Figure 2.- Comparison of exact and approximate values of the second derivative of the area distribution of configuration 3. The solid line indicates the exact values of S'' . The symbols indicate approximate values of S'' .